

Characterizing the composition and evolution of firework-related components in air aerosols during the Spring Festival

Keying Wu · Ming Duan · Hefan Liu · Zihang Zhou · Ye Deng · Danlin Song · Qinwen Tan

Received: 4 February 2018 / Accepted: 16 June 2018 / Published online: 22 June 2018
© Springer Nature B.V. 2018

Abstract To examine the impacts of fireworks, size-resolved PM samples were collected using a single-particle aerosol mass spectrometer before, during and after the Spring Festival in a megacity in Chengdu, China. Chemical composition and atmospheric behavior of urban particles were studied. Ten major single particle types were resolved with ART-2a algorithm including elemental and organic carbon (ECOC), EC, OC, levoglucosan (LEV), high molecular weight organic molecules (HOM), hard metal (HM), K rich, Na rich and SiO_3^- . The average OC/EC ratios decreased in the order AY (4.7) > overall (4.1) > NY (4.0) > BY period (3.6), indicating that many organic pollutants had been generated after the Spring Festival. The concentrations of many species exhibited an increasing trend during the firework period, and the SOR and NOR showed a strong increase in NY period. SOR and NOR had a slight positive relationship with fireworks activity but no obvious relationship with temperature.

Keywords Fireworks · SPMAS · $\text{PM}_{2.5}$ · Air pollution

Introduction

The Chinese Spring Festival is one of the most important traditional festivals in China. It is our traditional to set off firecrackers and fireworks to celebrate the Spring Festival in China. Tens of thousands of people set off firecrackers and fireworks at the same time, resulting in emission of huge volume of aerosols into the atmosphere in a short time (National-Statistics 2014). Though some success has been achieved in terms of pollution on implementation of air standards for firecrackers (Ye et al. 2013; He et al. 2014a, b), however, such strict emission control measures are not implemented in the Spring Festival in China.

Chengdu is a megacity which located in the plain of Sichuan basin (Wang et al. 2009), southwest China, and the economy has expanded rapidly in recently years (Xing et al. 2011). Because of its special geographical location, Chengdu has serious air pollution in winter, and much more attention has been drawn in particulate pollution in winter (Sufen 2009). As we all know, materials used in fireworks contain chemicals and toxic substances, burning of which release toxic gases and particulate matter of fine size to atmosphere leading to heavy air pollution (Wang et al. 2007).

K. Wu · M. Duan (✉)
Department of Chemistry and Chemical Engineering,
Southwest Petroleum University, No. 8 Xindu Road,
Chengdu 610500, People's Republic of China
e-mail: 18080498519@163.com

H. Liu · Z. Zhou · Y. Deng · D. Song · Q. Tan
Chengdu Academy of Environmental Sciences,
Chengdu 610000, People's Republic of China

Single-particle mass spectrometry (SPMAS) can detect real-time mixing state of the primary and secondary components of ambient PM, including refractory species like elemental carbon and trace metal (Li et al. 2011). Zhang et al. reported the composition and possible sources of PM_{2.5} particles based on single-particle aerosol mass spectrometer (SPAMS) measurements in Chengdu during the summer of 2016 (Zhang et al. 2017). However, particulate matter pollution in winter is much more serious than that of summer (Tian et al. 2012). The national government allows the burning of fireworks in the Spring Festival, and this provides the first opportunity to detect the associated changes in ambient air pollutant levels caused by fireworks using SPMAS. In this paper, we describe real-time single-particle analysis of Chengdu ambient air during the Spring Festival using SPAMS. PM_{2.5} samples of an extended festive period are chemically characterized for elements and ions, and these results are useful to understand the influence of fireworks display on Chengdu air quality.

Experimental methods

Sampling

The SPAMS (0525-R) (Li et al. 2011) used in this study was manufactured by Guangzhou Hexin Co., Ltd. (Guangzhou, China). Briefly, single particles with a size range of 0.1–3.0 µm are inhaled into a narrow beam through an aerodynamic lens and arrive at the sizing region. In the sizing region, two separated, diode-pumped Nd:YAG lasers ($\lambda = 532$ nm) are used to determine the vacuum aerodynamic diameter by measuring the time of flight of passing particles. Then, a Nd:YAG laser (266 nm, ~ 1 mJ/pulse, 1×10^8 W/cm², UL728F11-F115, Quantel, France) is used to desorb and ionize particles arriving at the mass spectrometer. The resulting positive and negative ions enter the flight tubes of the mass spectrometer and generate bipolar ion mass spectra. No industry exists within 20 km around the sampling site (104°3'15"E, 30°39'72"N). The instruments used in this study are installed on the stents of a car roof (8 m above ground).

The PM_{2.5} samples were pumped into the SPAMS inlet using size selectors connected to a conductive

silicone tube with an inner diameter of 6 mm and a length of ~ 2 m. A PM_{2.5} cyclone (URG, Corp., USA) was used to remove coarse particles, and a sampling pump was used to reduce the residence time of air in the sampling line. The meteorological data, including temperature, relative humidity (RH), wind speed and wind direction, were monitored from an automatic meteorological station (Vaisala MAWS201). Ambient NO_x (NO, NO₂) was monitored using a chemiluminescence nitrogen oxides analyzer (Thermo 42i). SO₂ and O₃ were monitored using Thermo 43i and Thermo 49i, respectively. PM mass was also measured using a Tapered Element Oscillating Microbalance (Thermo TEOM 1405) with a time resolution of 1 min. The mass concentrations of PM_{2.5} were measured using a SHARP 5030 instrument (Thermo, USA). Elemental carbon (EC) and organic carbon (OC) in PM_{2.5} were measured by a semi-continuous OC/EC analyzer (Sunset laboratory) using the thermal-optical transmittance method. Potentially toxic elements (PTE), detected by a Xact-625 heavy metal analyzer, were used to indicate the feature of trace apportionment, including K, Ca, Ba, Cu and Co.

Data analysis methods

All the single-particle spectra were imported to the YAADA toolkit (Software Toolkit to Analyze Single-Particle Mass Spectral Data, v 2.11). Particle clustering was performed with ART-2a adaptive resonance theory method (Song et al. 1999). The parameter setting for this analysis was: learning rate 0.05, vigilance factor 0.80 and iterations 20. Two hundred and seventy-six original groups were manually merged under the following conditions: (1) similar major ion pattern in the mass spectra and (2) similar temporal trend between particle types. Each particle cluster was named by its chemical composition, the clusters were then reduced to 10, which was used to describe the total SPAMS dataset, and others represent an unidentified group.

Results and discussion

Overview

The measurements period was 01/20/2017 (mm/dd/yyyy) to 01/31/2017. The temporal trends of

temperature, RH, NO₂, SO₂, O₃, PM_{2.5} and PM₁₀ are shown in Fig. 1. The average RH was 68 ± 12%. The wind was mainly from the north, northeast and northwest (Fig. 1), with a wind speed of 0.8 ± 0.7 m/s. The ratio of PM₁₀/PM_{2.5} was 0.62 ± 0.15; submicron particles were important during the Spring Festival period.

SPAMS clusters characterization

Ten kinds of average mass spectra of resolved particle types are shown in Fig. 2. Each cluster is named and identified according to its chemical composition.

EC The EC type includes carbon clusters, K⁺ (*m/z* 39), sulfate, and nitrate, Cl⁻, phosphate. And sulfate peaks are predominant in negative spectra.

ECOC The positive mass spectrum profile contains typical adjacent hydrocarbon ion fragments. This cluster is usually including carbenium ions, which

comes from an incomplete combustion process (Moffet and Prather 2009).

HM The average mass spectra of HM contain higher signal of heavy metal fragments, for example Pb(206, 207, 208), Zn(64, 66, 68), Cu(63, 65), As(75), Hg(202), Cr(52, 68), Mn(55), V(51,67) and Fe(54, 56). They have been attributed to coal burning emissions (Xu et al. 2012) and dust cluster (Silva et al. 2000).

HOC High mass HOC has a signal of the high molecule organic species such as C₈H₉⁺(*m/z* 105), C₁₀H₈⁺(*m/z* 128), C₁₃H₉⁺(*m/z* 165), C₁₄H₉⁺(*m/z* 177), C₁₅H₁₁⁺(*m/z* 191) and C₁₆H₁₀⁺(*m/z* 202) that are attributed to PAHs in ATOFMS study (Gross et al. 2000). The positive average mass spectra also contain carbon fragment C_n⁺ and hydrocarbon ion fragments including saturated hydrocarbon such as C_nH_{2n+1}⁺(*m/z* 43, 57, 71, etc.), unsaturated hydrocarbon C_nH_{2n-1}⁺(*m/z* 41, 55, 69, etc.) and oxidized species

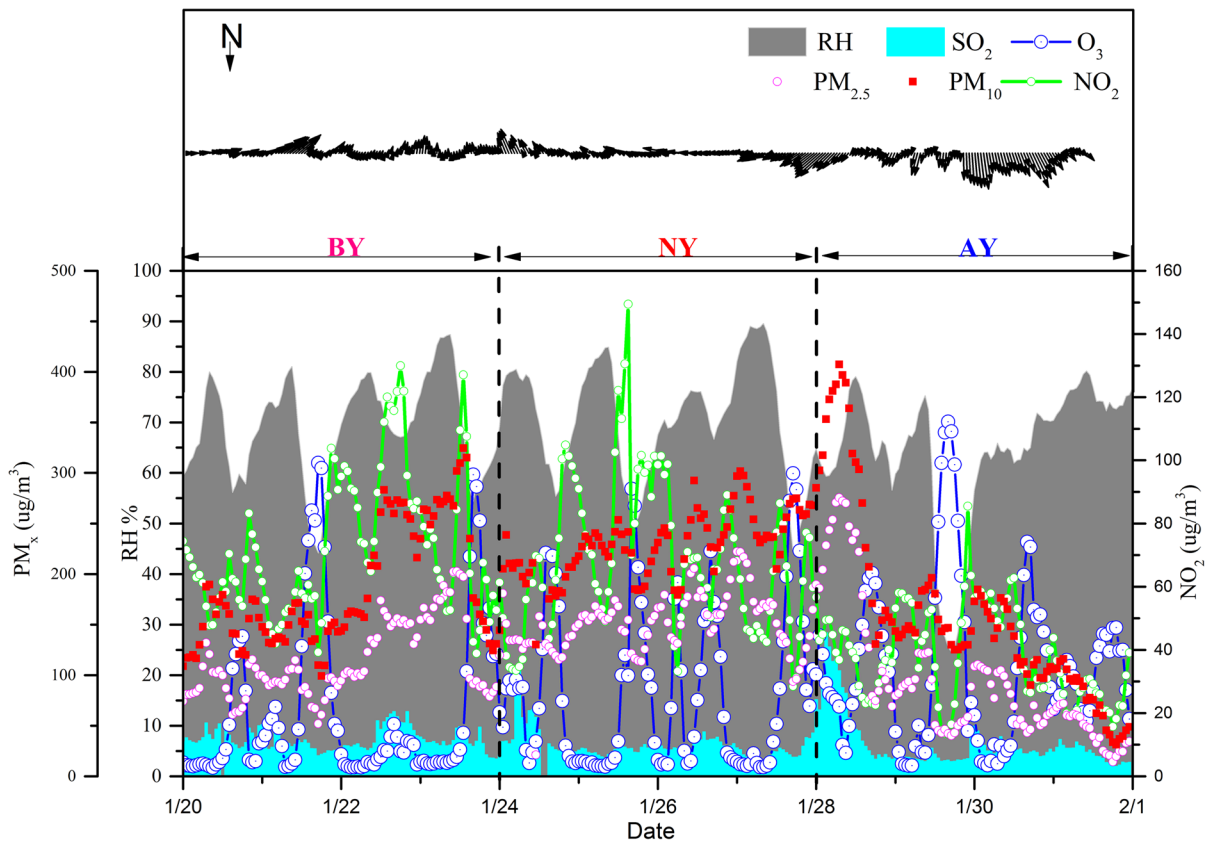


Fig. 1 Temporal trends of temperature, humidity, wind direct, wind speed, gaseous pollutants (SO₂, NO₂, PM_{2.5}, PM₁₀) in 1-h time resolution

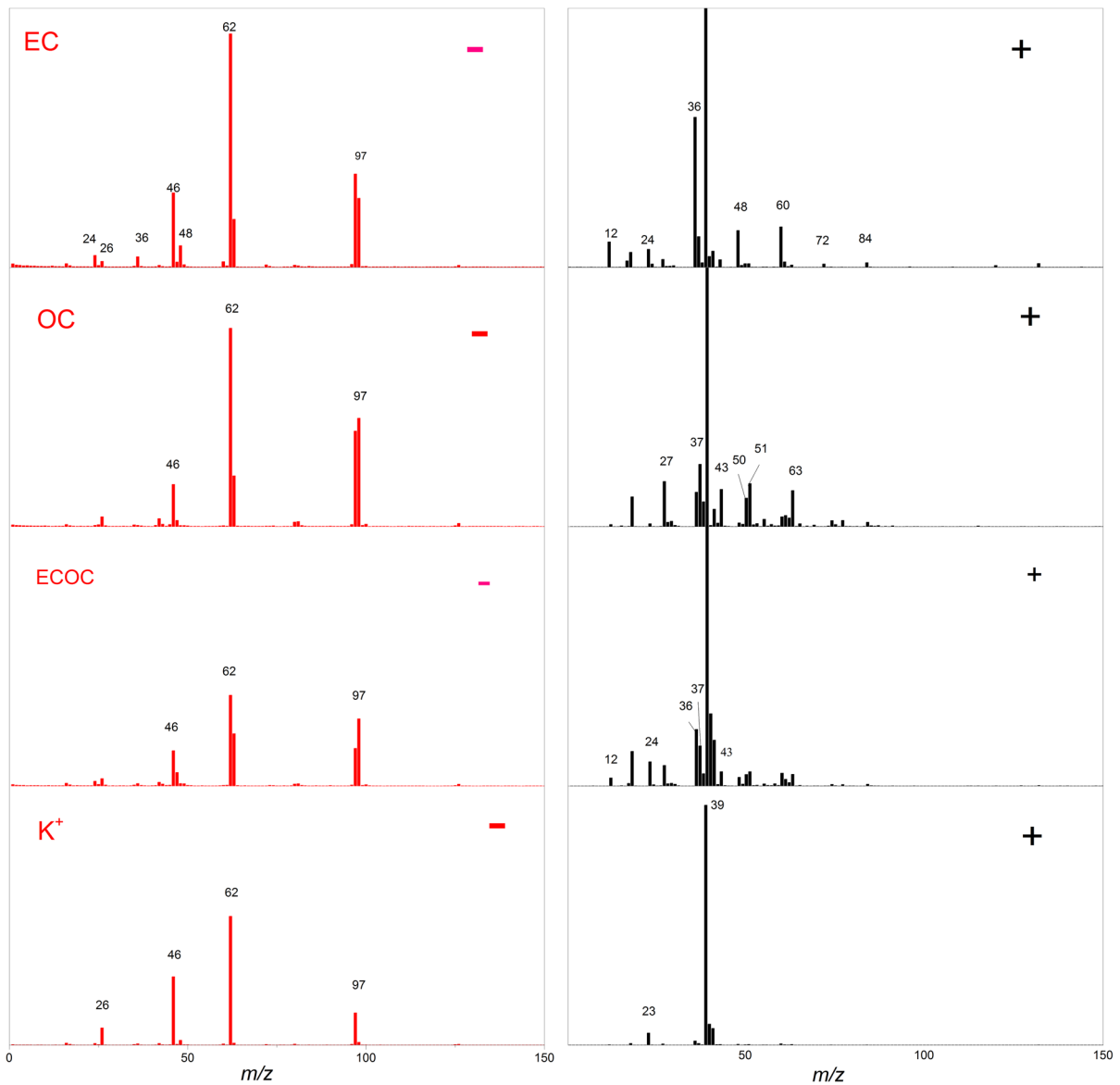


Fig. 2 Average mass spectra for single particle types in the Spring Festival SPAMS dataset. The label in each panel indicates the single particle type

like $C_xH_yO^+$ (m/z 42, $C_2H_2O^+$, m/z 59 $CH_3CO_2^+$). The negative ion spectrum contains carbon cluster, along with hydrocarbon ion fragments ($C_xH_y^-$), sulfate and nitrate.

K rich The average mass spectra of K rich contain higher signal of nitrate and sulfate and lower signal of Cl^- , CN^- , CNO^- than in the LEV average mass spectra.

LEV The positive mass spectrum contains the peak of K_2Cl^+ (113, 115) or $K_3SO_4^+$ (213, 215). In the

negative mass spectrum, sulfate (m/z 97, 80), nitrate (m/z 46 and 62), carbon (12, 24, 36, etc.), CN^- (m/z 26), Cl^- (m/z 35, 37) and CNO^- (m/z 42) are pronounced. The levoglucosan fragments are also found peaking at m/z 45, 59 and 71 (Silva et al. 1999). The levoglucosan particle type has also been reported in the previous studies (Bi et al. 2011; Dalosto and Harrison 2006; Healy et al. 2010; Moffet et al. 2008; Qin and Prather 2006).

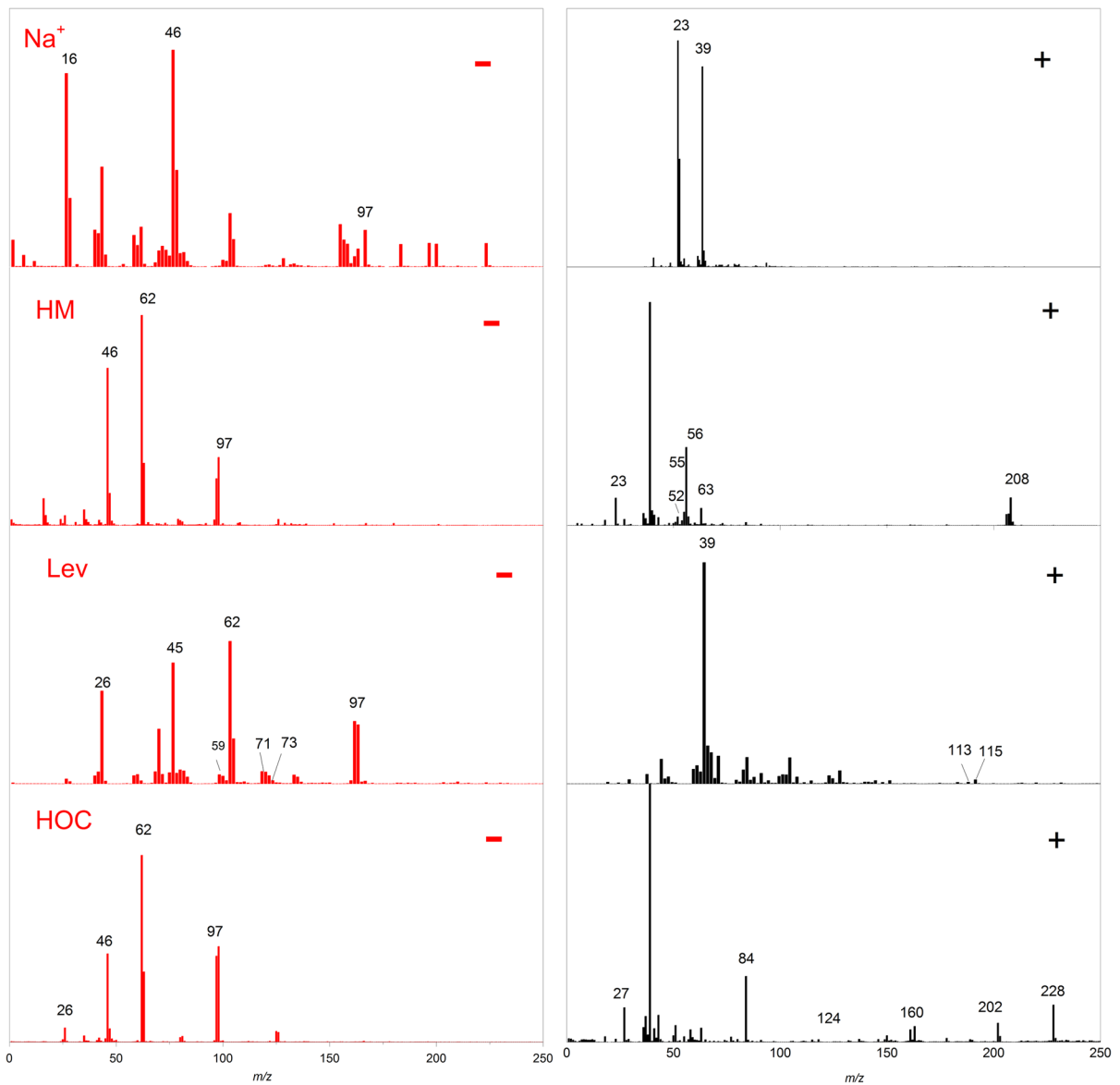


Fig. 2 continued

Na rich The organic species including hydrocarbon ion fragments, chloride and CN⁻ are notably lower than ECOC.

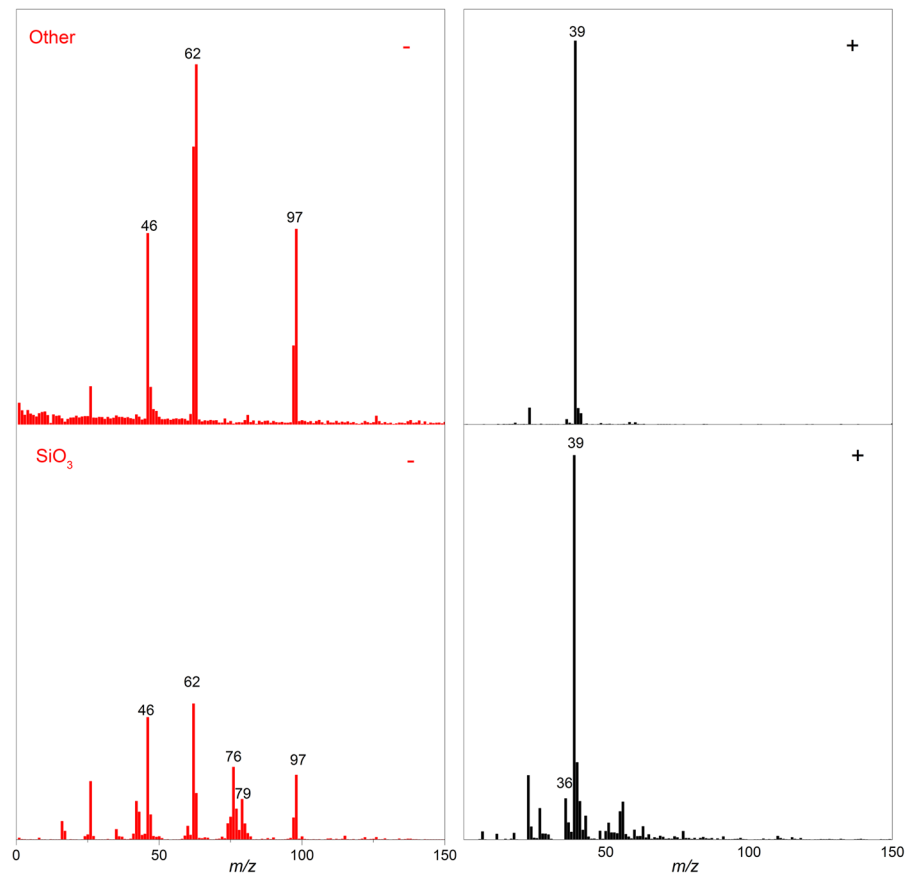
OC The OC particle type is characterized by abundant organic ion fragments, including C₂H₃⁺ (*m/z* 27), C₂H₅⁺ (*m/z* 29), C₃H⁺ (*m/z* 37), C₃H₃⁺ (*m/z* 39), C₂H₃O⁺ (*m/z* 43), and monoaromatic hydrocarbon peaks like 51, 63, 77 and 91 in the positive mass spectrum. C₂H⁻ (*m/z* 25), C₂H₂⁻ (*m/z* 26) and C₄H⁻ (*m/z* 49) are abundant in the negative spectrum.

Organic acid marker C₂H₅COO⁻/C₂HO₃⁻ (*m/z* 73) is also observed (Zauscher et al. 2013).

SiO₃ This particle is characterized with strong silicate and potassium peaks in the positive mass spectra. The silicate points to soil dust particles from building yards and unpaved roads that are common in some Chinese cities (Huang et al. 2014).

Other The positive mass spectrums contain the high abundance of other peaks, and we cannot classify them as one category.

Fig. 2 continued



Temporal trends of single-particle analysis

The temporal trends of single particle types can provide insights into the influence of fireworks display on variation of particle types during the Spring Festival period. As shown in Fig. 3, it is beginning to set off firecrackers in the morning of 01/27/2017. Average wind speed decreases below 0.5 m/s, and the humidity was 75%. Hourly PM₁₀ and PM_{2.5} mass concentration accumulated from 205 to 407 and 93 to 275 $\mu\text{g}/\text{m}^3$, respectively. Two severe haze episodes (BY and NY in Fig. 1) were characterized by high PM_{2.5} mass loadings. The first episode (BY) was from 01/20 to 01/24, when light haze accumulated gradually. The second episode (NY) was from 01/25 to 01/28, when quantities of firecrackers began setting off and severe haze occurred. The third episode (AY) was from 01/29 to 01/31, when the air becomes to be clear.

In NY, the count number of primary particle types like ECOC, K⁺ and OC increased. The aged groups,

such as K⁺, ECOC and secondary particle, also increased significantly after the Chinese New Year's Eve. These results suggest that the aged particle types were prominent during the Spring Festival period. In daytime, in the presence of light, pollutants get more space to disperse due to elevation of boundary layer height (Deka and Hoque 2014); what is more, fireworks activity is more intense. The formation of particulate event in Chengdu is driven by the accumulation of primary particles and formation of secondary particles.

Influence of fireworks on the physicochemical characteristics of PM pollution

Characteristics of fireworks

As shown in Fig. 4, concentrations of most species (such as crustal elements, heavy metal species, carbonaceous species, Cl⁻, K⁺ and Mg²⁺) exhibited increasing trends during the firework period. It is

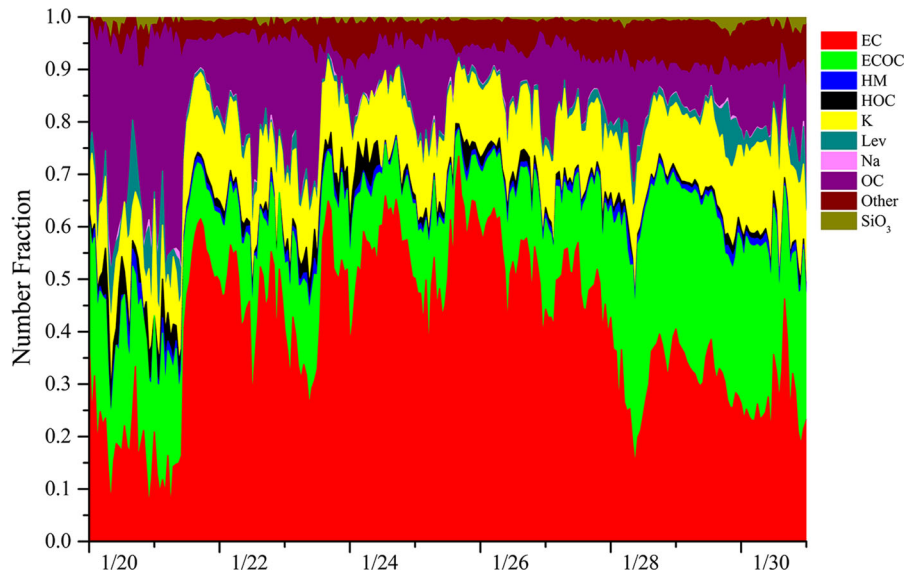


Fig. 3 Unscaled time-resolved number fraction of single-particle clusters

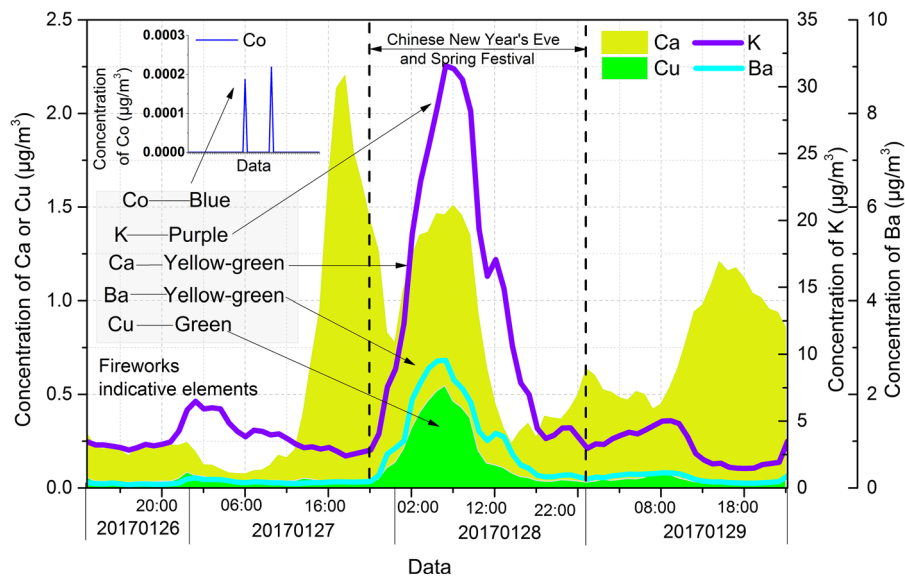


Fig. 4 Concentrations of K, Ca, Ba, Cu, Co in the atmosphere during the observation

believed that Ca, Co, Cu, Ba, Cl^- , K^+ and Mg^{2+} might represent firework-related species. Potassium is one of the major components of fireworks because potassium compounds in black powder (commonly in the form of perchlorate or chlorate) act as the main oxidisers during burning, with the corresponding chemical equations being $2\text{KClO}_3 = 2\text{KCl} + 3\text{O}_2$ and $\text{KClO}_4 = \text{KCl} + 2\text{O}_2$. The Ca compounds (such as calcium chloride and sulfate), Ba compounds and Cu

compounds (such as copper chloride and oxide) give rise to orange and blue color, respectively. (Conkling 1985). A Cr compound (CuCr_2O_4) is used as a catalyst for propellants. Cu, K, and Co are used to provide silvery and glitter effects as well. Many components are in the form of perchlorate or chlorate (Munster et al. 2009). Leading to high concentrations of Cl^- , the abruptly high emissions of these elements due to firework combustion can explain the high

concentrations of these firework-related species in atmospheric PM during the Spring Festival period. It is noteworthy that certain firework-related heavy metals (Co, Ba, Cu, etc.) are dangerous elements because of their toxicity and are forbidden by law in many countries (Vecchi et al. 2008). Such high concentrations in a short time, especially in a place where a considerable number of people are gathered, might be of concern. Apparently, a fivefold increase in mass concentration of heavy metals is observed during the Spring Festival Eve.

The temporal variations of the carbonaceous species and the ratio of OC/EC for 20–31 January are shown in Fig. 5. In this study, the average values of OC on the BY, NY and AY episode were 30.9, 37.1 and 17.0 $\mu\text{g}/\text{m}^3$, respectively. The average values of EC in three episodes were 8.8, 9.3 and 3.8 $\mu\text{g}/\text{m}^3$, respectively.

On the other hand, the ratio of OC/EC has been used as a valuable tool to indicate the sources and formation of carbonaceous aerosol. The previous studies have shown that the OC/EC ratios for vehicle emissions, coal combustion and biomass burning were 0.7–2.4, 0.3–7.6 and 4.1–14.5 (Watson et al. 2001; Qin and Xie 2011), respectively. A study of Chinese sources similarly showed that the OC/EC ratios from coal combustion and biomass burning are much higher than those from vehicle emissions (Gan et al. 2010). In this study, the average OC/EC ratios decreased in the order

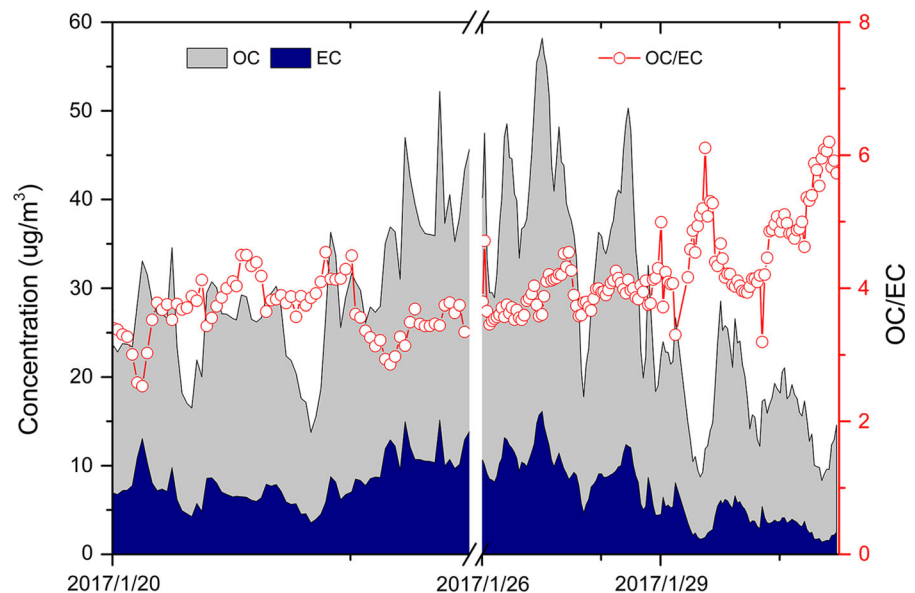
AY (4.7) > overall (4.1) > NY (4.0) > BY period (3.6), indicating that many organic pollutants had generated after the Spring Festival. The average OC and EC in $\text{PM}_{2.5}$ were 28.9 and 7.5 mg/m^3 in the whole observation period, respectively, lower than the corresponding value in other studies (Cao et al. 2007) in Beijing (OC = 27.1 mg/m^3 ; EC = 7.1 mg/m^3), Shanghai (OC = 28.6 mg/m^3 ; EC = 8.3 mg/m^3) and Guangzhou (OC = 41.1 mg/m^3 ; EC = 14.5 mg/m^3).

Intense secondary aerosol transformation

It is noteworthy that fireworks contain many toxicity heavy metals, such high concentrations in a short time, especially in a place where a considerable number of people are gathered, might be of concern. Except for the directly firework-related species, an increase was also observed for most of the inorganic elements (such as S, K and N).

Additionally, the sulfur oxidation ratio ($\text{SOR} = n\text{SO}_4^{2-}/(n\text{SO}_4^{2-} + n\text{SO}_2)$, n is the molar concentration) and nitrogen oxidation ratio ($\text{NOR} = n\text{NO}_3^-/(n\text{NO}_3^- + n\text{NO}_2)$) were important factors; their high values show that gaseous species were oxidized to secondary aerosols in the atmosphere (Sun et al. 2006). It has been reported that SOR is less than 0.10 in primary source emissions (Pierson et al. 1979) but higher than 0.10 when sulfate is produced through the photochemical oxidation of SO_2 (Ohta and

Fig. 5 Time series of carbonaceous species and ratio of OC/EC during the observation



Okita 1990). Overall, the SOR and NOR in both NY and AY (Fig. 6b) showed strong secondary aerosol transformation. Especially, in Spring Festival’s Eve, quantities of fireworks display in a short time, releasing a lot of SO₂. And the high levels of SOR and NOR led to rapid accumulation of sulfates and nitrates, resulting in worsening of the haze pollution. SOR was always larger than NOR, and thus, the concentration of SO₄²⁻ was higher than that of NO₃⁻ all the time (Fig. 6a). The highest SOR (0.85) occurred at 8:00 on 27 January; 23 h later, the highest

concentration of PM_{2.5} (275 mg/m³) in AY was observed.

The average NORs were elevated slightly from 0.28 (AY) to 0.30 (NY), and NOR showed a clearly increasing trend in both AY and NY. The averages of SOR in AY and NY were 0.61 and 0.70, respectively, the same trend as the NOR. Figure 6b shows that NOR/SOR and NO₃⁻/SO₄²⁻ both had increase trends with event development, especially during NY. NOR/SOR showed a positive correlation with NO₃⁻/SO₄²⁻, as their variation was similar. SOR showed a slightly

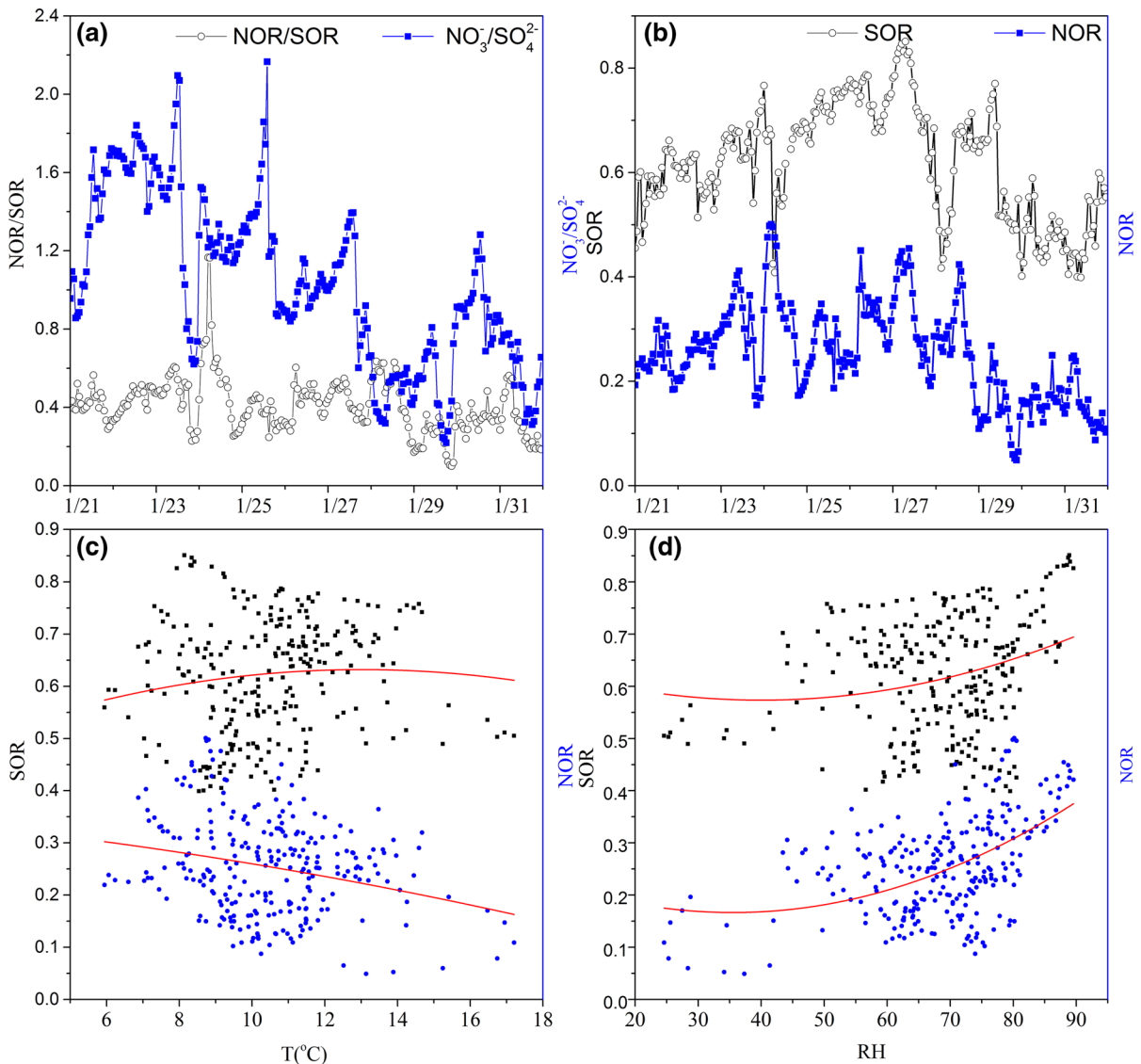


Fig. 6 Time series of **a** NOR/SOR and NO₃⁻/SO₄²⁻ and **b** SOR and NOR during the observation, and the relationship and curve fitting between **c** temperature and SOR or NOR, and **d** RH and SOR or NOR

more increasing trend; the increase in NOR was important for the increase trend of $\text{NO}_3^-/\text{SO}_4^{2-}$ in NY.

SOR and NOR showed a strong interrelationship in AY. SO_4^{2-} is predominantly formed by homogeneous gas-phase reactions of SO_2 with OH radicals and heterogeneous reactions in the aqueous surface layer of preexisting particles and in-cloud processes (Meng and Seinfeld 1994; Yao et al. 2002). The formation of NO_3^- from NO_2 usually occurs via a homogeneous gas-phase reaction of NO_2 with OH radicals and heterogeneous chemistry involving the hydrolysis of dinitrogen pentoxide on aerosol surfaces (Pathak et al. 2008). Additionally, it has been reported that high levels of NO_x might accelerate the reaction from SO_2 to SO_4^{2-} (He et al. 2014a, b). Thus, the formation of both SO_4^{2-} and NO_3^- is largely related to heterogeneous chemistry. However, NOR and SOR have almost no relationship in NY (Fig. 6d). It is possible that the oxidation mechanism may have been different in the two episodes. The concentration of O_3 was extremely low in BY (Fig. 1), indicating that the photochemical reaction was not strong and atmospheric oxidation was insufficient during BY, which was a restrictive condition for SOR and NOR, even though the gas precursors are abundant.

SOR and NOR showed no obvious relation to temperature (Fig. 6c); the very low temperature may have provided little enhancement to them. SOR and NOR showed an increasing trend with increased RH (Fig. 6d), which implied that high RH was conducive to the conversion of SO_2 to SO_4^{2-} and NO_2 to NO_3^- .

Conclusions

To quantify the direct impacts of fireworks, size-resolved PM samples were collected in a megacity in Chengdu. An online measurement of urban single particle types was taken in Chengdu during the Spring Festival of 2017 from 01/20 to 01/31. The major particle types were mainly carbonaceous particles and metal-rich dust. The sampling campaign covered the Spring Festival, which provides a unique opportunity to quantify the contributions of fireworks under significantly different emission patterns. The strong influence of fireworks on the physicochemical characteristics of atmospheric $\text{PM}_{2.5}$ was observed. During the observation period, intense secondary pollutant transformation

was observed; the SOR and NOR showed a strong interrelationship in NY period. SOR and NOR had a slight positive relationship with fireworks activity but no obvious relationship with temperature. However, NOR and SOR have almost no relationship in NY. It is possible that the oxidation mechanism may have been different in the two episodes.

Acknowledgements The financial support from “Atmospheric pollution emissions inventory of Chengdu in 2017 [No. HKY2017009-3]” and “Chengdu Key Laboratory of Atmospheric Research” is acknowledged.

References

- Bi, X., Zhang, G., Li, L., Wang, X., Li, M., & Sheng, G. (2011). Mixing state of biomass burning particles by single particle aerosol mass spectrometer in the urban area of PRD, China. *Atmospheric Environment*, 45, 3447–3453.
- Cao, J. J., Lee, S. C., Chow, J. C., Watson, J. G., Ho, K. F., Zhang, R. J., et al. (2007). Spatial and seasonal distributions of carbonaceous aerosols over China. *Journal Geophysical Research*, 112, 2–11.
- Conkling, J. A. (1985). *Chemistry of pyrotechnics: Basic principles and theory*. New York, NY: Marcel Dekker Inc.
- Dalosto, M., & Harrison, R. (2006). Chemical characterisation of single airborne particles in Athens (Greece) by ATOFMS. *Atmospheric Environment*, 40, 7614–7631.
- Deka, P., & Hoque, R. R. (2014). Diwali fireworks: Early signs of impact on PM_{10} properties of rural Brahmaputra Valley. *Aerosol and Air Quality Research*, 14(6), 1752–1762.
- Gan, Z., Li, J., Li, X. D., Yue, X., Guo, L. L., Tang, J. H., et al. (2010). Impact of anthropogenic emissions and open biomass burning on regional carbonaceous aerosols in South China. *Environmental Pollution*, 158, 3392–3400.
- Gross, D. S., Galli, M. E., Silva, P. J., & Prather, K. A. (2000). Relative sensitivity factors for alkali metal and ammonium cations in single-particle aerosol time-of-flight mass spectra. *Analytical Chemistry*, 72, 416–422.
- He, G. Y., Luo, B., Chen, J. W., Zhang, W., Liao, Q. Y., & Liu, P. C. (2014a). The impact of fireworks on air quality during the spring festival in Chengdu downtown area. *Sichuan Environment*, 1, 014.
- He, H., Wang, Y., Ma, Q., Ma, J., Chu, B., Ji, D., et al. (2014b). CORRIGENDUM: Mineral dust and NO_x promote the conversion of SO_2 to sulfate in heavy pollution days. *Scientific Reports*, 4, 4172.
- Healy, R. M., Hellebust, S., Kourtchev, I., Allanic, A., O’Connor, I. P., & Bell, J. M. (2010). Source apportionment of $\text{PM}_{2.5}$ in Cork Harbour, Ireland using a combination of single particle mass spectrometry and quantitative semi-continuous measurements. *Atmospheric Chemistry and Physics*, 10, 9593–9613.
- Huang, R. J., Zhang, Y., Bozzetti, C., Ho, K. F., Cao, J. J., Han, Y., et al. (2014). High secondary aerosol contribution to particulate pollution during haze events in China. *Nature*, 514, 218–222.

- Li, L., Huang, Z. X., Dong, J. G., Li, M., Gao, W., Nian, H. Q., et al. (2011). Real time bipolar time-of-flight mass spectrometer for analyzing single aerosol particles. *International Journal of Mass Spectrometry*, *303*, 118–124.
- Meng, Z., & Seinfeld, J. H. (1994). On the source of the sub-micrometer droplet mode of urban and regional aerosols. *Aerosol Science and Technology*, *20*, 253–265.
- Moffet, R. C., de Foy, B., Molina, L. T., Molina, M. J., & Prather, K. A. (2008). Measurement of ambient aerosols in northern Mexico City by single particle mass spectrometry. *Atmospheric Chemistry and Physics*, *8*, 4499–4516.
- Moffet, R. C., & Prather, K. A. (2009). In-situ measurements of the mixing state and optical properties of soot with implications for radiative forcing estimates. *Proceedings of the National Academy of Sciences of the United States of America*, *106*, 11872–11877.
- Munster, J., Hanson, G. N., Jackson, W. A., & Rajagopalan, S. (2009). The fallout from fireworks: perchlorate in total deposition. *Water, Air, and Soil pollution*, *198*(1–4), 149–153.
- National-Statistics. (2014). *Chengdu statistics 2014*. Beijing: China Statistics Press.
- Ohta, S., & Okita, T. (1990). A chemical characterization of atmospheric aerosol in Sapporo. *Atmospheric Environment*, *24*, 815–822.
- Pathak, R. K., Wu, W. S., & Wang, T. (2008). Summertime PM_{2.5} ionic species in four major cities of China: Nitrate formation in an ammonia-deficient atmosphere. *Atmospheric Chemistry and Physics*, *9*, 1711–1722.
- Pierson, W. R., Brachaczek, W. W., & Mckee, D. E. (1979). Sulfate emissions from catalyst equipped automobiles on the highway. *Journal of the Air and Waste Management Association*, *29*, 255–257.
- Qin, Y., & Xie, S. D. (2011). Historical estimation of carbonaceous aerosol emissions from biomass open burning in China for the period 1990–2005. *Environmental Pollution*, *159*, 3316.
- Silva, P. J., Carlin, R. A., & Prather, K. A. (2000). Single particle analysis of suspended soil dust from Southern California. *Atmospheric Environment*, *34*, 1811–1820.
- Song, X. H., Hopke, P. K., Fergenson, D. P., & Prather, K. A. (1999). Classification of single particles analyzed by ATOFMS using an artificial neural network, ART-2 A. *Analytical Chemistry*, *71*, 860–865.
- Sufen, G. (2009). Application progresses on controlled atmosphere grain storage technology by purging nitrogen. *Grain Storage*, *4*, 005.
- Sun, Y., Zhuang, G., Tang, A., Wang, Y., & An, Z. (2006). Chemical characteristics of PM_{2.5} and PM₁₀ in Haze-Fog episodes in Beijing. *Environmental Science and Technology*, *40*, 3148.
- Tian, H. Z., Lu, L., Cheng, K., Hao, J. M., Zhao, D., & Wang, Y. (2012). Anthropogenic atmospheric nickel emissions and its distribution characteristics in China. *Science of the Total Environment*, *417*, 148–157.
- Vecchi, R., Bernardoni, V., Cricchio, D., D'Alessandro, A., Fermo, P., Lucarelli, F., et al. (2008). The impact of fireworks on airborne particles. *Atmospheric Environment*, *42*(6), 1121–1132.
- Wang, F., Cheng, Q., Highland, L., Miyajima, M., Wang, H., & Yan, C. (2009). Preliminary investigation of some large landslides triggered by the 2008 Wenchuan earthquake, Sichuan Province, China. *Landslides*, *6*(1), 47–54.
- Wang, Y., Zhuang, G. S., Xu, C., & An, Z. S. (2007). The air pollution caused by the burning of fireworks during the lantern festival in Beijing. *Atmospheric Environment*, *41*, 417–431.
- Watson, J. G., Chow, J. C., & Houck, J. E. (2001). PM_{2.5} chemical source profiles for vehicle exhaust, vegetative burning, geological material, and coal burning in North-western Colorado during 1995. *Chemosphere*, *43*(8), 1141–1151.
- Xing, X., Qi, S., Zhang, J., Wu, C., Zhang, Y., Yang, D., et al. (2011). Spatial distribution and source diagnosis of polycyclic aromatic hydrocarbons in soils from Chengdu Economic Region, Sichuan Province, western China. *Journal of Geochemical Exploration*, *110*(2), 146–154.
- Xu, H., Cao, J., Ho, K., Ding, H., Han, Y., Wang, G., et al. (2012). Lead concentrations in fine particulate matter after the phasing out of leaded gasoline in Xi'an. *China Atmospheric Environment*, *46*, 217–224.
- Yao, X., Chan, C. K., Fang, M., Cadle, S., Chan, T., Mulawa, P., et al. (2002). The water-soluble ionic composition of PM_{2.5} in Shanghai and Beijing. *China Atmospheric Environment*, *36*, 4223–4234.
- Ye, L., You, H., Yao, J., Kang, X., & Tang, L. (2013). Seasonal variation and factors influencing perchlorate in water, snow, soil and corns in Northeastern China. *Chemosphere*, *90*(10), 2493–2498.
- Zauscher, M. D., Wang, Y., Moore, M. J., Gaston, C. J., & Prather, K. A. (2013). Air quality impact and physico-chemical aging of biomass burning aerosols during the 2007 San Diego wildfires. *Environmental Science and Technology*, *47*, 7633–7643.
- Zhang, J., Luo, B., Zhang, J., Ouyang, F., Song, H., Liu, P., et al. (2017). Analysis of the characteristics of single atmospheric particles in Chengdu using single particle mass spectrometry. *Atmospheric Environment*, *157*, 91–100.